

# Remarkable Effects of Axial $\pi^*$ Coordination on the Cr–Cr Quadruple Bond in Dichromium Paddlewheel Complexes

F. Albert Cotton,<sup>\*,†</sup> Lee M. Daniels,<sup>†</sup> Carlos A. Murillo,<sup>\*,†,‡</sup> Isabel Pascual,<sup>†</sup> and Hong-Cai Zhou<sup>†</sup>

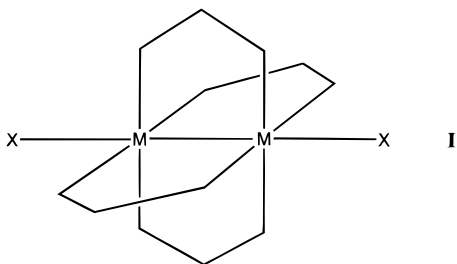
Contribution from The Laboratory for Molecular Structure and Bonding, Department of Chemistry, P.O. Box 30012, Texas A&M University, College Station, Texas 77842-3012, and Escuela de Química, Universidad de Costa Rica, Ciudad Universitaria, Costa Rica

Received April 20, 1999

**Abstract:** It is well-known that donation of electron density into the  $\sigma^*$  orbital of a Cr–Cr quadruple bond causes major lengthening of the Cr–Cr distance, and there is some prior evidence that a similar lengthening is caused by dative interaction with the  $\pi^*$  orbitals. Some molecules have now been made that allow a definitive assessment of this axial  $\pi^*$  effect. A molecule has been designed to ensure that there is axial donation into the  $\pi^*$  orbitals but not onto the  $\sigma^*$  orbital; ligands have been used in which the donor atoms are tethered to the bridging ligands in such a way that they can reach only the  $\pi^*$  orbitals but not the  $\sigma^*$  orbital. The ligands used for this purpose are the anions of 2,6-di(phenylimino)piperidine (DPhIP) and 2,2'-dipyridylamine (dpa). In the compound  $\text{Cr}_2(\text{DPhIP})_4$  four imino nitrogen lone pairs are suitably positioned to donate to the  $\pi^*$  orbitals and the Cr–Cr bond length is 2.265(1) Å. For direct comparison, the compound  $\text{Cr}_2(\text{PhIP})_4$  (PhIP is the anion of 2-(phenylimino)piperidine) was made and found to have a Cr–Cr distance of 1.858(1) Å. In this case the ligand is very similar to DPhIP except that it has no donor nitrogen atoms available for axial  $\pi^*$  donation. Thus, the cumulative effect of donation from four nitrogen atoms is very large, namely, 0.4 Å in the Cr–Cr distance. The  $\text{Cr}_2(\text{dpa})_4$  molecule occurs in three different crystalline compounds, in all of which there are slightly different conformations, but the same Cr–Cr distance,  $1.94 \pm 0.01$  Å; these may be compared to that in the compound  $\text{Cr}_2(\text{mpa})_4$  (1.87 Å) in which the bridging is quite similar but there are no tethered additional donor atoms.

## Introduction

A fundamental and recurring question concerning the M–M distances in complexes of the type  $\text{M}_2\text{L}_4\text{X}_n$ , where M is one of a number of transition metal atoms, L is a bridging bidentate ligand (e.g.,  $\text{RCO}_2^-$ ), and X is an axial ligand (of which there may be 0, 1, or 2), is the extent to which these distances are influenced by the identity of M, the nature of L, and the presence of X.<sup>1</sup> It is for compounds of chromium<sup>1b</sup> that this question arises in its most acute form, since Cr–Cr distances range from 1.83 to 2.60 Å depending on L, X, and  $n$ , all within the common structural motif of the paddlewheel arrangement of the four L ligands (I).



It has been argued<sup>1b</sup> that while the Cr–Cr distances are certainly sensitive to the identity of the ligand L, they are much more sensitive to axial ligation. In most previous discussions, an axial ligand has been assumed to be a  $\sigma$ -donor, but in one

case<sup>2</sup>  $\pi$  donation was found to be predominant. In this case molecules of  $\text{Cr}_2(\text{O}_2\text{CCPh}_3)_4$  have benzene axially coordinated with the ring planes perpendicular to the Cr–Cr axis. The Cr–Cr distance is 2.26 Å, which may be compared with a value of 1.97 Å found for the  $\text{Cr}_2(\text{O}_2\text{CCH}_3)_4$  molecule in the gas phase.<sup>3</sup> Calculations showed clearly that the lengthening was attributable to donation of electron density from the benzene  $e_{1g}$  orbitals to the  $\pi^*$  orbitals of the  $\text{Cr}_2$  unit. A subsequent attempt to develop the concept in more detail had only limited success, but did provide further support.<sup>4</sup> More recently, we have reported<sup>5</sup> that in certain molecules there are weak interactions between  $o$ -fluorine atoms on ligands and the chromium atoms that seem to be responsible for modest increases (0.07–0.11 Å) in the Cr–Cr distance. From the molecular structures, it was not easy to say whether these interactions were of  $\pi^*$  or  $\sigma^*$  character, or both. In any case, these results reawakened our interest in axial interaction of the  $\pi^*$  type and motivated us to seek ligands that would be capable of introducing such interactions in an explicit and major way.

(1) (a) Cotton, F. A.; Walton, R. A. *Multiple Bonds Between Metal Atoms*, 2nd ed.; Oxford University Press: Oxford, England, 1993. (b) Cotton, F. A.; Walton, R. A. *Multiple Bonds Between Metal Atoms*, 2nd ed.; Oxford University Press: Oxford, England, 1993; Chapter 4. (c) Cotton, F. A.; Walton, R. A. *Multiple Bonds Between Metal Atoms*, 2nd ed.; Oxford University Press: Oxford, England, 1993; Chapter 7.

(2) Cotton, F. A.; Feng, X.; Kibala, P. A.; Matusz, M. *J. Am. Chem. Soc.* **1988**, *110*, 2807.

(3) Ketkar, S. N.; Fink, M. *J. Am. Chem. Soc.* **1985**, *107*, 338.

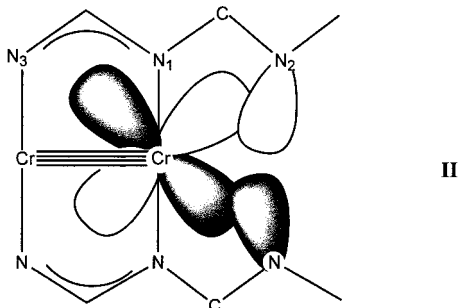
(4) Cotton, F. A.; Daniels, L. M.; Kibala, P. A. *Inorg. Chem.* **1992**, *31*, 1865.

(5) Cotton, F. A.; Murillo, C. A.; Pascual, I. *Inorg. Chem.* **1999**, in press.

<sup>†</sup> Texas A&M University.

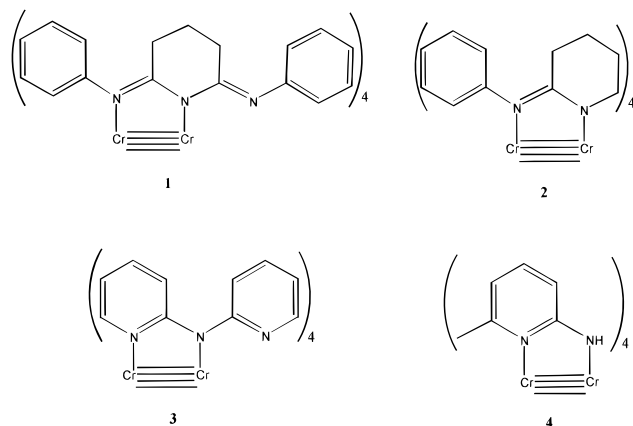
<sup>‡</sup> University of Costa Rica.

Thus, in this report we are concerned with new, and we believe definitive, examples that show how donation of electrons to the  $\pi^*$  orbitals can weaken and thus lengthen the Cr–Cr bond. The examples we present here are quite different from anything previously reported. Here the donors are nitrogen atoms appended to the bridging ligands in such a way that their lone pair electrons are positioned where the distal lobes of the  $\pi^*$  orbitals are expected to be, as shown schematically in **II**.



The diagram **II** shows a situation in which donation from the filled lone pair orbitals on appropriately tethered nitrogen atoms into the empty  $\pi^*$  lobes of the chromium atoms is maximal. Two deviations from this situation can lessen the interaction: (1) The Cr...N distances may increase as a result of increases in the N–C–N angles. (2) The lone-pair orbitals may become “misdirected” as the torsional angles Cr–N1–C–N2 deviate from  $0^\circ$ , that is, as the N2 atom deviates from the plane defined by Cr–N1–C. To avoid confusion of these angles with the torsional angles about the Cr–Cr bonds, we shall call these “direction angles”. We shall comment further on the role of these factors after the actual compounds and their structures have been described.

The complexes with which this work has been carried out are shown schematically as **1–4**. Compound **2** is a reference



compound for **1**. In **2**, where the ligand is the 2-phenyliminopiperidinate anion, PhIP, no axial  $\pi^*$  interactions can occur, whereas in **1**, where the ligand is the 2,6-di(phenylimino)piperidinate anion, DPhIP, four such interactions occur, two at each end of the molecule. Compound **4**, whose structure has previously been reported<sup>9</sup> is a reference for compound **3**, which has also been reported<sup>7</sup> earlier in one crystal form (**3**·DMF) and is now reported here in two more.

## Experimental Section

**General Procedures.** All manipulations were carried out under nitrogen using standard Schlenk techniques. Solvents were purified by conventional methods, and were freshly distilled under nitrogen prior to use. Anhydrous  $\text{CrCl}_2$  was purchased from Strem Chemicals and stored in a drybox; MeLi (1.0 M in THF/cumene) was purchased from Aldrich and used as received; Hdpa (2,2'-dipyridylamine) was obtained from Aldrich and sublimed before use; HDPHIP, 2,6-di(phenylimino)piperidine, and HPhIP, 2-(phenylimino)piperidine, were synthesized following published procedures.<sup>8,9</sup> Infrared spectral data were recorded on KBr pellets using a Perkin-Elmer 16 PC FT-IR spectrometer; NMR spectra were recorded on a Varian XL-200 spectrometer. Elemental analyses were performed by Canadian Microanalytical Services Ltd.; they were satisfactory.

**Preparation of  $\text{Cr}_2(\text{DPhIP})_4$  (**1**).** The compound HDPHIP (1.06 g, 4.0 mmol) was dissolved in THF (5.0 mL) and cooled to  $-78^\circ\text{C}$ . Then MeLi in THF/cumene (1.0 M, 4.2 mL) was added dropwise. Bubbles quickly formed, and a pale yellow solution was obtained. Anhydrous  $\text{CrCl}_2$  (0.26 g, 2.0 mmol) was then added through a solids addition tube. The resulting yellow suspension was then stirred at room temperature for 3 h. A yellow solid was collected by a filtration and washed with THF (5.0 mL) and hexanes ( $3 \times 10$  mL). Additional product was obtained from workup of the filtrate. The filtrate and THF wash solution were combined and mixed with hexanes (30 mL), resulting in a yellow solid. This solid was dissolved in  $\text{CH}_2\text{Cl}_2$  (10.0 mL) and filtered to remove LiCl; the resulting reddish solution was evacuated to dryness under vacuum, leaving a yellow product. The solids were combined; crystallization from warm THF afforded **1**·2THF as a yellow crystalline solid (0.850 g, 65.5%).  $^1\text{H}$  NMR ( $\text{CD}_2\text{Cl}_2$ ,  $\delta$ ): 6.73 (m, 8H), 5.71 (m, 2H), 2.77 (m, 4H), 2.58 (m, 2H). IR (KBr,  $\text{cm}^{-1}$ ): 1655 (w), 1623 (w), 1579 (w), 1492 (w), 1440 (s), 1370 (m), 1346 (m), 1319 (w), 1261 (w), 1217 (s), 1192 (m), 1072 (w), 1026 (m), 905 (w), 866 (w), 803 (m), 762 (m), 699 (s), 601 (w), 511 (m), 420 (w). Recrystallization of **1** from THF/hexanes generated red crystals of **1**·THF. Recrystallization of **1**·THF or **1**·2THF from either  $\text{CH}_2\text{Cl}_2$ /hexanes or  $\text{CH}_2\text{Cl}_2$ /diethyl ether afforded red crystals of **1**· $\text{CH}_2\text{Cl}_2$ .

**Preparation of  $\text{Cr}_2(\text{PhIP})_4$  (**2**).** The compound HPhIP (0.38 g, 2.2 mmol) was dissolved in toluene (15 mL), deprotonated by MeLi at  $-78^\circ\text{C}$ , and added to  $\text{CrCl}_2$  (0.14 g, 1.1 mmol). The reaction mixture first became yellow and then orange. This orange suspension was refluxed for 1 h, then stirred at room temperature overnight. The resulting dark red solution was filtered through Celite to remove LiCl and layered with hexanes. Needle-shaped yellow (1 mm) crystals grew in two weeks. Yield: 0.065 g (15%).  $^1\text{H}$  NMR ( $\text{C}_6\text{D}_6$ ,  $\delta$ ): 7.12 (t, 2H), 6.89 (t, 1H), 6.52 (d, 2H), 2.86 (t, 2H), 2.62 (t, 2H), 1.43 (m, 4H). IR (KBr,  $\text{cm}^{-1}$ ): 1593 (m), 1571 (m), 1547 (vs), 1522 (w), 1518 (w), 1508 (w), 1488 (vs), 1458 (m), 1438 (w), 1425 (w), 1400 (w), 1389 (w), 1376 (w), 1355 (m), 1327 (w), 1317 (w), 1274 (s), 1261 (s), 1234 (s), 1178 (w), 1155 (w), 1117 (s), 1088 (m), 1065 (m), 1026 (m), 959 (m), 909 (w), 892 (w), 856 (w), 800 (s), 756 (m), 704 (s), 695 (m), 670 (w), 661 (w), 618 (w), 594 (w), 522 (w), 492 (w), 474 (w), 448 (w), 420 (w), 412 (w).

**Preparation of  $\text{Cr}_2(\text{dpa})_4$  (**3**).** The compound Hdpa (0.34 g, 2.0 mmol) dissolved in 15 mL of THF was deprotonated with an equivalent amount of MeLi. To the colorless suspension, at  $-78^\circ\text{C}$ , were added 0.24 g (1.5 mmol) of anhydrous  $\text{CrCl}_2$  through a solids addition tube. The suspension quickly turned red. It was kept at low temperature to avoid conversion to  $\text{Cr}_3(\text{dpa})_4\text{Cl}_2$ ,<sup>9</sup> which is green in color. After 2 h of stirring, the red suspension was filtered while cold. A red solid was isolated, washed with THF, and dried under vacuum. It was recrystallized from  $\text{CH}_2\text{Cl}_2$ /hexanes as red crystals of **3**·2 $\text{CH}_2\text{Cl}_2$ . It was also crystallized from a solution in THF/hexanes as red needle-shaped crystals of **3**. Crystalline yield: 0.32 g (56%).  $^1\text{H}$  NMR ( $\text{CD}_2\text{Cl}_2$ ,  $\delta$ ): 8.16 (d, 1H), 7.52 (d, 1H), 7.42 (d, 1H), 7.29 (m, 3H), 6.97 (d, 1H), 6.01 (d, 1H). IR (KBr,  $\text{cm}^{-1}$ ): 1603 (vs), 1580 (vs), 1560 (s), 1487–1421 (br, vs), 1376 (s), 1284 (s), 1255 (s), 1172 (m), 1016 (s), 986 (m), 946 (w), 921 (w), 877 (w), 835 (w), 769 (s), 747 (s), 731 (s), 535

(6) Cotton, F. A.; Niswander, R. H.; Sekutowski, J. C. *Inorg. Chem.* **1978**, *17*, 3541.

(7) Edema, J. J. H.; Gambarotta, S.; Meetswa, A.; Spek, A. L.; Smeets, W. J. J.; Chiang, M. Y. *J. Chem. Soc., Dalton Trans.* **1993**, 789.

(8) Elvidge, J. A.; Linstead, R. P.; Salaman, A. M. *J. Chem. Soc.* **1959**, 208.

(9) Bredereck, H.; Bredereck, K. *Chem. Ber.* **1961**, 2779.

**Table 1.** Crystal Data and Structure Refinement<sup>a</sup>

complex	1·THF	1·2THF	1·CH <sub>2</sub> Cl <sub>2</sub>	2	3	3·2CH <sub>2</sub> Cl <sub>2</sub>
chem formula	C <sub>72</sub> H <sub>72</sub> N <sub>12</sub> Cr <sub>2</sub> O	C <sub>76</sub> H <sub>74</sub> Cr <sub>2</sub> N <sub>12</sub> O <sub>2</sub>	C <sub>69</sub> H <sub>66</sub> N <sub>12</sub> Cr <sub>2</sub> Cl <sub>2</sub>	C <sub>44</sub> H <sub>52</sub> N <sub>8</sub> Cr <sub>2</sub>	C <sub>40</sub> H <sub>32</sub> N <sub>12</sub> Cr <sub>2</sub>	C <sub>42</sub> H <sub>36</sub> N <sub>12</sub> Cl <sub>4</sub> Cr <sub>2</sub>
fw	1225.42	1291.47	1238.24	796.94	784.775	954.63
space group	<i>I</i> 2/ <i>a</i>	<i>P</i> $\bar{1}$	<i>I</i> 2/ <i>a</i>	<i>P</i> $\bar{1}$	<i>C</i> 2/ <i>c</i>	<i>C</i> 2/ <i>c</i>
<i>a</i> , Å	27.2495(8)	14.198(2)	27.197(3)	9.8649(7)	18.100(4)	23.966(6)
<i>b</i> , Å	16.486(2)	14.638(7)	16.467(8)	10.1338(8)	11.706(2)	9.581(2)
<i>c</i> , Å	29.413(2)	18.12(1)	29.51(1)	20.561(3)	16.595(3)	19.106(4)
<i>a</i> , deg	90	108.97(2)	90	77.59(2)	90	90
$\beta$ , deg	110.416(5)	109.53(4)	110.43(2)	80.50(2)	102.48(3)	104.763(5)
$\gamma$ , deg	90	95.27(3)	90	81.14(1)	90	90
<i>V</i> , Å <sup>3</sup>	12384(1)	3270(3)	12385(7)	1964.9(3)	3433(1)	4242(2)
<i>Z</i>	8	2	8	2	4	4
<i>T</i> , K	213(2)	213(2)	213(2)	213(2)	213(2)	213(2)
radiation $\lambda$ , Å	0.71073	0.71073	0.71073	0.71073	0.71073	0.71073
$\rho$ (calcd), g cm <sup>-3</sup>	1.315	1.312	1.333	1.347	1.518	1.495
$\mu$ (Mo K $\alpha$ ), cm <sup>-1</sup>	4.10	3.90	4.90	6.00	6.85	8.12
R1 <sup>b</sup> /R1 <sup>c</sup>	0.058/0.075	0.060/0.072	0.070/0.091	0.049/0.056	0.069/0.100	0.051/0.056
wR2 <sup>b</sup> /wR2 <sup>c</sup>	0.132/0.155	0.147/0.159	0.160/0.189	0.117/0.126	0.133/0.156	0.125/0.132

<sup>a</sup>R1 =  $\sum(|F_o| - |F_c|)/\sum|F_o|$ . wR2 =  $[\sum w[(F_o^2 - F_c^2)^2]/\sum w(F_o^2)]^{1/2}$ ;  $w = 1/[\sigma^2(F_o^2) + (a \cdot P)^2 + b \cdot P]$ ,  $P = [\max(F_o^2 \text{ or } 0) + 2(F_c^2)]/3$ . <sup>b</sup>Denotes the value of the residual considering only the reflections with  $I > 2\sigma(I)$ . <sup>c</sup>Denotes value of the residual considering all the reflections.

**Table 2.** Selected Bond Lengths (Å) and Angles (deg) for Cr<sub>2</sub>(DPhIP)<sub>4</sub> in 1·THF

Cr(1)–Cr(2)	2.2652(9)	Cr(2)–N(3)	2.111(3)
Cr(1)–N(2)	2.063(3)	Cr(2)–N(5)	2.065(3)
Cr(1)–N(6)	2.103(3)	Cr(2)–N(9)	2.097(3)
Cr(1)–N(8)	2.060(3)	Cr(2)–N(11)	2.063(3)
Cr(1)–N(12)	2.124(3)		
N(2)–Cr(1)–Cr(2)–N(3)	9.1(1)	N(6)–Cr(1)–Cr(2)–N(5)	7.6(1)
N(8)–Cr(1)–Cr(2)–N(9)	7.6(1)	N(12)–Cr(1)–Cr(2)–N(11)	7.4(1)
Cr(1)···N(1)	2.745(3)	Cr(2)···N(4)	2.945(3)
Cr(1)···N(7)	2.809(3)	Cr(2)···N(10)	2.738(3)
Cr(1)–N(2)–C(7)–N(1)	6.3(4)	Cr(2)–N(5)–C(24)–N(4)	0.9(4)
Cr(1)–N(8)–C(41)–N(7)	2.7(4)	Cr(2)–N(11)–C(58)–N(10)	2.2(4)

(m), 518 (w), 446 (m), 410 (m). Mass spectroscopy (FAB<sup>+</sup>, NBA as matrix, *m/z*): 784, [Cr<sub>2</sub>(dpa)<sub>4</sub>]<sup>+</sup>; 614, [Cr<sub>2</sub>(dpa)<sub>3</sub>]<sup>+</sup>; 565, [Cr(dpa)<sub>3</sub>]<sup>+</sup>; 392, [Cr(dpa)<sub>2</sub>]<sup>+</sup>; 273, [Cr<sub>2</sub>(dpa)]<sup>+</sup>.

**Crystallographic Studies.** Data collection for all crystals was carried out on a Nonius Fast area detector diffractometer with each crystal mounted on the tip of a glass fiber under a stream of nitrogen. All data sets were collected at –60 °C. Cell parameters were obtained by least-squares refinement of 250 reflections ranging in 2 $\theta$  from 15° to 41°. Laue groups and centering conditions were confirmed by axial images. Data were collected using 0.2° intervals in  $\varphi$  for the range 0° <  $\varphi$  < 220° and 0.2° intervals in  $\omega$  for two different regions in the range 0° <  $\omega$  < 72°. In this way, nearly a full sphere of data was collected. The highly redundant data sets were corrected for Lorentz and polarization effects, and for absorption.

The positions of the chromium atoms and their first coordination spheres were determined by direct methods and refined by using the program SHELXL-93. All non-hydrogen atoms were found by successive iterations of least-squares refinement followed by Fourier syntheses and, during the final cycles, were refined anisotropically. Hydrogen atoms were placed in idealized positions, and a common thermal parameter was refined. In 2·2THF, the disordered phenyl rings were modeled in two orientations each, and refined at half occupancy for each orientation.

Crystallographic data for 1·THF, 1·2THF, 1·CH<sub>2</sub>Cl<sub>2</sub>, 2, 3, and 3·2CH<sub>2</sub>Cl<sub>2</sub> are given in Table 1. Selected bond distances and angles for 1·THF (structural parameters of 1·CH<sub>2</sub>Cl<sub>2</sub> are very similar to those of 1·THF) are given in Table 2. Selected bond distances and angles for 1·2THF, 2, and 3 (structural parameters for 3·2CH<sub>2</sub>Cl<sub>2</sub> are very similar to those of 3) are found in Tables 3, 4 and 5, respectively.

## Results and Discussion

**Remarks Regarding Syntheses.** The ligand DPhIP has three nitrogen donors. It is structurally similar to the dpa ligand,<sup>10</sup> so

**Table 3.** Selected Bond Lengths (Å) and Angles (deg) for Cr<sub>2</sub>(PhIP)<sub>4</sub>, 2

Cr(1)–Cr(1A)	1.858(1)	Cr(1)–N(2)	2.050(3)
Cr(1A)–N(1)	2.057(3)	Cr(1A)–N(4)	2.053(3)
Cr(1)–N(3)	2.050(3)		
Cr(1)–Cr(1A)–N(1)	98.55(8)	Cr(1A)–Cr(1)–N(2)	92.67(8)
Cr(1A)–Cr(1)–N(3)	94.77(8)	Cr(1)–Cr(1A)–N(4)	96.16(8)
N(1)–Cr(1)–N(2)	116.7(3)	N(3)–Cr(1)–N(4)	116.0(3)
N(1)–Cr(1A)–Cr(1)–N(2)	0.1(1)	N(4)–Cr(1A)–Cr(1)–N(3)	3.4(1)

**Table 4.** Selected Bond Lengths (Å) and Angles (deg) for Cr<sub>2</sub>(DPhIP)<sub>4</sub> in 1·2THF

Cr(1)–Cr(2)	2.155(1)	Cr(2)–N(3)	2.115(3)
Cr(1)–N(2)	2.034(3)	Cr(2)–N(5)	2.056(3)
Cr(1)–N(6)	2.128(3)	Cr(2)–N(9)	2.097(3)
Cr(1)–N(8)	2.073(3)	Cr(2)–N(11)	2.046(3)
Cr(1)–N(12)	2.112(3)		
N(2)–Cr(1)–Cr(2)–N(3)	10.9(1)	N(6)–Cr(1)–Cr(2)–N(5)	13.1(1)
N(8)–Cr(1)–Cr(2)–N(9)	12.1(1)	N(12)–Cr(1)–Cr(2)–N(11)	10.1(1)
Cr(1)···N(1)	2.734(3)	Cr(2)···N(4)	2.881(3)
Cr(1)···N(7)	3.057(3)	Cr(2)···N(10)	2.935(3)
Cr(1)–N(2)–C(7)–N(1)	10.8(4)	Cr(2)–N(5)–C(24)–N(4)	2.5(4)
Cr(1)–N(8)–C(41)–N(7)	9.4(4)	Cr(2)–N(11)–C(58)–N(10)	0.4(4)

it can also support linear trimetallic chains.<sup>11</sup> Control of stoichiometry and reaction temperature are crucial to the product distribution. When the molar ratio of LiDPhIP and CrCl<sub>2</sub> is 2:1, and the reaction is carried out in THF at room temperature, 1 is formed exclusively. If the molar ratio of LiDPhIP and CrCl<sub>2</sub> is higher than 2:1, and the reaction is carried out at reflux temperature, a mixture of 1 and a green trichromium complex is formed.<sup>12</sup> Compound 1 is moderately soluble in THF, and very soluble in CH<sub>2</sub>Cl<sub>2</sub>, but insoluble in benzene or acetonitrile. It can be recrystallized from THF/hexanes as red crystals of 1·THF and from hot THF as orange crystals of 1·2THF. Compound 1 can also be recrystallized from CH<sub>2</sub>Cl<sub>2</sub>/hexanes or CH<sub>2</sub>Cl<sub>2</sub>/ether as red block-crystals of 1·CH<sub>2</sub>Cl<sub>2</sub>. The solutions of 1 are air sensitive, but the crystalline forms of 1 are surprisingly stable. For example, 1·THF as red crystals has been kept in air for two months without noticeable change in appearance or crystal structure.

(10) Cotton, F. A.; Daniels, L. M.; Murillo, C. A.; Pascual, I. *Inorg. Chem. Commun.* **1998**, 1, 1.

(11) Cotton, F. A.; Daniels, L. M.; Murillo, C. A.; Pascual, I. *J. Am. Chem. Soc.* **1997**, 119, 10223.

(12) The green trichromium complex will be described elsewhere.

**Table 5.** Structural Parameters of **1**·THF and **1**·2THF Related to Axial Coordination

<b>1</b> ·THF [Cr–Cr (Å): 2.2652(9)]				<b>1</b> ·2THF [Cr–Cr (Å): 2.155(1)]			
direction angles (deg)		Cr···N (Å)		direction angles (deg)		Cr···N (Å)	
Cr(2)–N(11)–C(58)–N(10)	2.2(3)	Cr(2)···N(10)	2.738(3)	Cr(1)–N(2)–C(7)–N(1)	10.8(4)	Cr(1)···N(1)	2.734(3)
Cr(1)–N(2)–C(7)–N(1)	6.3(4)	Cr(1)···N(1)	2.745(3)	Cr(2)–N(5)–C(24)–N(4)	2.5(4)	Cr(2)···N(4)	2.881(3)
Cr(1)–N(8)–C(41)–N(7)	2.7(4)	Cr(2)···N(7)	2.809(3)	Cr(2)–N(11)–C(58)–N(10)	0.4(3)	Cr(2)···N(10)	2.935(3)
Cr(2)–N(5)–C(24)–N(4)	0.9(4)	Cr(2)···N(4)	2.945(3)	Cr(1)–N(8)–C(41)–N(7)	9.4(4)	Cr(2)···N(7)	3.057(3)
$\Sigma$	12(2)		11.24(2)	$\Sigma$	23(2)		11.61(2)

The preparation methods for dichromium paddlewheel complexes with various bidentate ligands can vary greatly depending on the solubility and basicity of the ligand. Carboxylate ligands can be deprotonated with NaOMe, and can react with  $\text{Cr}_2(\text{CH}_3\text{COO})_4 \cdot 2\text{H}_2\text{O}$  in ethanol or aqueous solution. Hydroxypyridine can be neutralized with butyllithium in THF and reacts with  $\text{Cr}_2(\text{CH}_3\text{COO})_4$ . Chromocene is also an excellent starting material, when the ligand is insufficiently soluble.<sup>13</sup> When a formamidinate-type ligand is used,  $\text{CrCl}_2$  can be allowed to react with the lithiated ligand in THF.<sup>14</sup> HPhIP is structurally similar to a formamidinate, and it is even soluble in petroleum ether. Instead of THF, toluene was used for the reaction between  $\text{CrCl}_2$  and LiPhIP. The reaction mixture was refluxed for 1 h to ensure a complete conversion. A toluene solution of **2** was obtained by a single filtration which removed LiCl and a small amount of an impurity.

The most remarkable thing we have observed in the preparative chemistry concerning compound **1** is the structural diversity. We have obtained it in three crystalline forms: **1**·THF, **1**· $\text{CH}_2\text{Cl}_2$ , and **1**·2THF. The first two (which are isomorphous) are red, whereas the last one is orange. The color difference, red vs orange, is striking and immediately prompts the question of how the “same” molecule can have two quite different colors when only the kind or number of solvent molecules is changed. It is well-known<sup>1c</sup> that  $\text{Rh}_2(\text{O}_2\text{CCH}_3)_4 \cdot \text{S}_2$  compounds vary a great deal in color as the solvent molecules, S, are varied, but this is a case where the solvent molecules are directly coordinated to the  $\text{Rh}_2(\text{O}_2\text{CCH}_3)_4$  molecules in axial positions. As we shall see shortly, in all of the three differently solvated forms of compound **1**, the solvent molecules are simply interstitial, having no specific interaction with the chromium atoms.

**The Evidence for  $\pi^*$  Interactions.** We begin with **1**·THF, which crystallizes in space group  $I2/a$  with all atoms in general positions. No significant intermolecular interactions were found. A drawing of the molecule in **1**·THF is shown in Figure 1. There are four DPhIP anions bridging a dichromium unit. Each ligand uses two of its three nitrogen atoms to coordinate equatorially with the dichromium unit. The third nitrogen is dangling, but located near one of the two chromium atoms in an off-axis position. The directions of the four pendant arms of the ligands alternate around the dichromium unit. The distances between the pendant nitrogen atoms and the closest chromium atoms are listed in Table 2. The striking feature of molecule **1** in **1**·THF is the Cr–Cr distance of 2.265(9) Å, which is the longest Cr–Cr distance in any paddlewheel complex supported only by nitrogen donor ligands.

We attribute the remarkable elongation of the Cr–Cr bond to the interaction between the lone pair of pendant nitrogen atoms and the  $d_{xz}$  and  $d_{yz}$  orbitals of the two chromium atoms. One way to look at this interaction is shown in Figure 2, which is a schematic molecular orbital diagram showing the interactions of a metal  $d_{yz}$  orbital and two such nitrogen lone pairs.

We see a group orbital composed of the two nitrogen lone pairs, which matches the symmetry of the  $d_{yz}$  orbital of a chromium atom, interacts with the  $d_{yz}$  orbital, and results in a half-occupied antibonding orbital. This antibonding orbital then interacts with the  $d_{yz}$  orbital of the other chromium atom to form a destabilized  $\pi$ -bonding orbital. The  $d_{xz}$  orbital of the other chromium atom in a molecule of  $\text{Cr}_2(\text{DPhIP})_4$  also interacts with the other two nitrogen atoms in exactly the same way. These interactions pull the Cr atoms apart causing the elongation of the Cr–Cr bond. An alternative way to formulate the situation is to regard the pendant nitrogen atoms as donating into the  $\pi^*$  orbital in the Cr–Cr bond, thus canceling some of the  $\pi$  bonding. Table 6 shows that the sum of the direction angles of **1** in **1**·THF is only 12(2)°, so the lone pair orbitals of nitrogen atoms point almost directly to the empty  $\pi^*$  lobes of the chromium atoms. In addition, the Cr···N distances are short; they vary from 2.74 to 2.95 Å, with a sum of 11.24 Å for the four ligands in the molecule. This is the explanation we propose for the long Cr–Cr distance of 2.265(1) Å that is found in **1**·THF.

To check on the correctness of this explanation other experiments were carried out. The first one was the following. We prepared a compound as similar as possible to **1**, except that the pendant nitrogen atoms that we claim are responsible for the lengthening of the Cr–Cr bond are absent. This is compound **2**, and its actual structure is shown in Figure 3. The molecular dimensions are listed in Table 3, and it can be seen that there is an enormous change in the Cr–Cr distance, which has shrunk from 2.265(1) Å to 1.858(1) Å, while no other significant changes have occurred.

While we believe that the case is proven by the results just presented, we are pleased that there is more supporting evidence. One such piece is especially welcome because it came unexpectedly. The reader will recall that in addition to **1**·THF and its isomorph **1**· $\text{CH}_2\text{Cl}_2$ , both of which are red solids, we obtained the orange solid **1**·2THF. Let us now look at the structure of **1**·2THF. Superficially, the molecule of **1** present closely resembles the one found in **1**·THF, but (Table 4) a critical difference is immediately obvious: the Cr–Cr distance is about 0.10 Å shorter, namely, 2.155(1) Å compared to 2.265(1) Å. How can the “same” molecule show such a structural difference in two different crystal forms? Once again, we see the exquisite sensitivity of the Cr–Cr bond to axial interactions at play, only now we are looking at  $\pi^*$  instead of  $\sigma^*$  interactions.

According to our previous reasoning in explaining the difference between the Cr–Cr distances in **1**·THF and **2** we look for a difference in the axial interactions occurring in the molecule **1** in **1**·THF and **1**·2THF, and as Table 5 shows, we find exactly what is needed to explain the Cr–Cr bond length difference. While the sum of the four Cr···N distances is only slightly longer in **1**·2THF the nitrogen lone pairs are far more “misdirected” than they are in **1**·THF. Therefore, there is much less donation into the  $\text{Cr}_2 \pi^*$  orbitals and the Cr–Cr distance is much less elongated, namely by only about 0.3 Å instead of 0.4 Å.

(13) Cotton, F. A.; Thompson, J. L. *Inorg. Chem.* **1981**, *20*, 1292.(14) Cotton, F. A.; Ren, T. *J. Am. Chem. Soc.* **1992**, *114*, 2237.

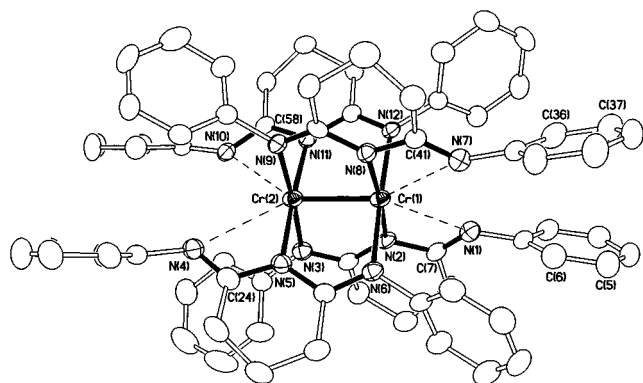


**Figure 1.** A drawing of the molecular structure of  $[\text{Cr}_2(\text{DPhIP})_4]$  in  $1 \cdot \text{THF}$ . Thermal displacement ellipsoids are drawn at 50% probability. Hydrogen atoms have been omitted for clarity. The axial  $\pi^*$  interactions are also shown.

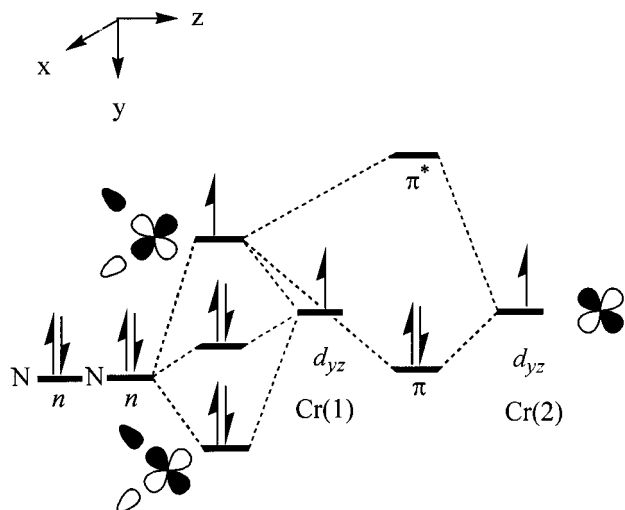


**Figure 2.** Schematic MO diagram showing the effect of axial coordination from an appendage of a bridging ligand.

Our reasoning so far suggests an obvious question. If it is only molecular packing forces that cause the axial  $\pi^*$  interactions to change in going from  $1 \cdot \text{THF}$  to  $1 \cdot 2\text{THF}$ , will the structural difference not vanish in solution? To answer this question we made solutions in  $\text{CD}_2\text{Cl}_2$  from both kinds of crystals and showed that they have identical  $^1\text{H}$  NMR spectra. The spectrum is shown in Figure 4. Moreover, the colors of the two solutions were visually indistinguishable. In fact we were able to learn a little more about the structure in solution from the  $^1\text{H}$  NMR spectrum. It appears that it must be rather similar to that shown in Figure 1 for  $1 \cdot \text{THF}$ . Another view of that structure is shown as a space-filling model in Figure 5. Here it can be seen that on each end of the molecule the phenyl groups in the pendant  $\text{NCC}_6\text{H}_5$  groups have a very particular spatial relationship to each other. They are close (3.44 Å from C(6) to C(36)), almost parallel, but offset so that only two hydrogen atoms of each one, those on C(36), C(37) and C(5), C(6), lie right over the plane of the other ring. In such positions and at such close distances we should expect these four protons (eight altogether for the whole molecule) to experience a distinct upfield shift relative to the others. That is exactly what Figure 4 shows. Most of the aromatic resonances lie in their usual region, 6.5–7.0 ppm, but there is a signal at 5.7 ppm due to the eight that are shifted by the diamagnetic anisotropy of the neighboring phenyl rings. The intensity ratio observed agrees within experimental error with that expected, 4:1. It may also

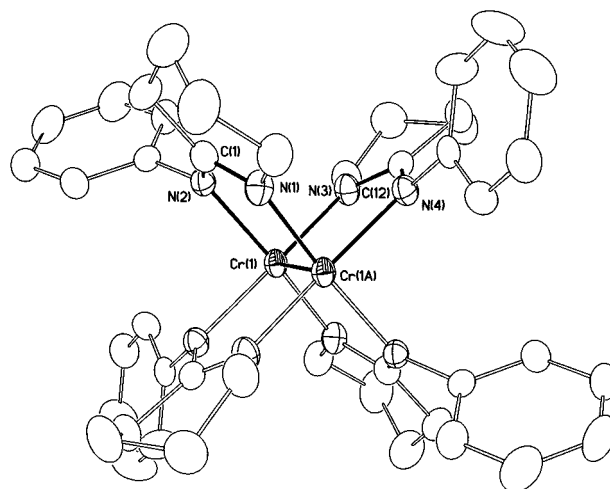


**Figure 3.** A drawing of  $\text{Cr}_2(\text{PhIP})_4$ , **2**. Ellipsoids are drawn at the 50% probability level. Hydrogen atoms have been omitted for clarity.

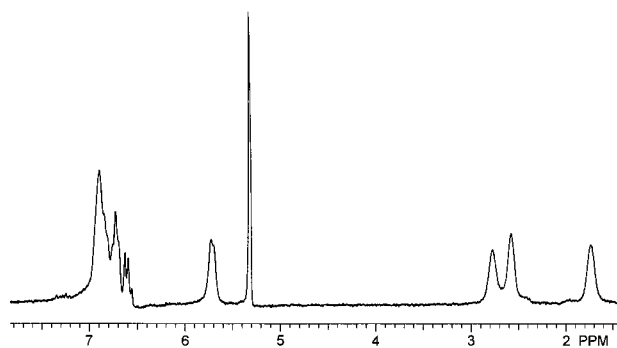


**Figure 4.**  $^1\text{H}$  NMR spectrum of  $\text{Cr}_2(\text{DPhIP})_4$  in  $\text{CD}_2\text{Cl}_2$  showing a signal shifted from the normal aromatic region (6.5–7.0 ppm) to 5.7 ppm. The signal at 5.3 ppm is from the solvent.

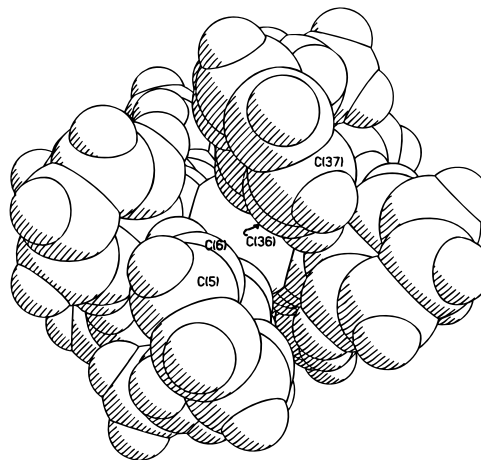


**Figure 5.** Space filling model of  $\text{Cr}_2(\text{DPhIP})_4$  in  $1 \cdot \text{THF}$  showing the shielding of two protons on each end phenyl ring by the opposite phenyl group.

be noted that because of the unsymmetrical relationship of each DPhIP ligand to the  $\text{Cr}_2$  unit, there are three methylene signals.

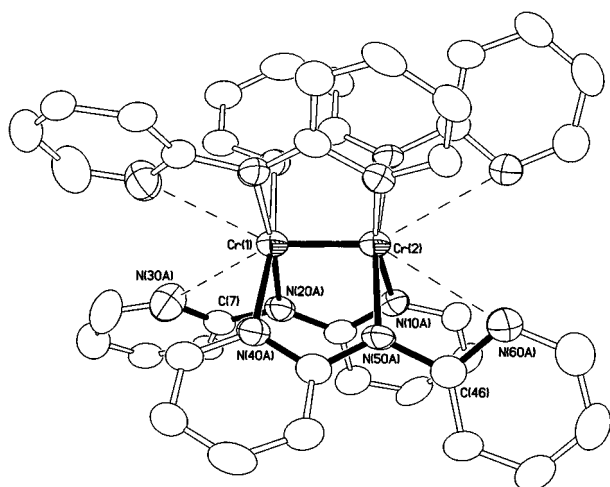
There is still more experimental evidence to adduce in favor of the influence of axial  $\pi^*$  interactions on Cr–Cr bond lengths. For this we turn to the  $\text{Cr}_2(\text{dpa})_4$  molecule, **3**,  $3 \cdot 2\text{CH}_2\text{Cl}_2$ , and previously<sup>7</sup>  $3 \cdot \text{DMF}$  (DMF = dimethylformamide). Our results for **3** are shown in Figure 6 and Table 6. Results for all three cases are found in Table 7, where the structural features pertaining to axial interaction are presented. The Cr–Cr distance

**Table 6.** Selected Bond Lengths (Å) and Angles (deg) for **3**

Cr(1)–Cr(2)	1.943(2)		
Cr(1)–N(20A)	2.068(5)	Cr(2)–N(10A)	2.062(5)
Cr(1)–N(40A)	2.075(5)	Cr(2)–N(50A)	2.040(5)
N(10A)–Cr(2)–Cr(1)–N(20A)	4.1(2)	N(50A)–Cr(2)–Cr(1)–N(40A)	6.0(2)
Cr(1)···N(30A)	2.751(6)	Cr(2)···N(60A)	3.089(6)
Cr(1)–N(20A)–C(7)–N(30A)	11.4(6)	Cr(2)–N(50A)–C(46)–N(60A)	40.4(7)

**Table 7.** Structural Parameters of **3**, **3**·2CH<sub>2</sub>Cl<sub>2</sub>, and **3**·DMF<sup>a</sup> Related to Axial Coordination

<b>3</b> [Cr–Cr (Å): 1.943(2)]		<b>3</b> ·2CH <sub>2</sub> Cl <sub>2</sub> [Cr–Cr (Å): 1.940(1)]		<b>3</b> ·DMF <sup>a</sup> [Cr–Cr (Å): 1.935]	
direction angles (deg)	Cr–N (Å)	direction angles (deg)	Cr–N (Å)	direction angles (deg)	Cr–N (Å)
11.4(6)	2.751(6)	24.7(4)	2.820(3)	23.4	2.865
11.4(6)	2.751(6)	24.7(4)	2.820(3)	23.4	2.865
40.4(7)	3.089(6)	37.1(4)	3.022(4)	32.0	2.955
40.4(7)	3.089(6)	37.1(4)	3.022(4)	32.0	2.955
$\Sigma$	104(3)	$\Sigma$	124(2)	$\Sigma$	111
	11.68(3)		11.68(2)		11.64

<sup>a</sup> See reference 7.**Figure 6.** A drawing of Cr<sub>2</sub>(dpa)<sub>4</sub>, **3**. Ellipsoids are drawn at the 50% probability level. Hydrogen atoms have been omitted for clarity. The possible axial  $\pi^*$  interactions are also shown.

is almost invariant in these three structures, being virtually constant at  $1.940 \pm 0.005$  Å. This may be compared with the value in the reference compound **4**, where it is 1.87 Å. This elongation can also be attributed to axial  $\pi^*$  interactions.

It can be seen in Figure 6 that in Cr<sub>2</sub>(dpa)<sub>4</sub> there are axial  $\pi^*$  interactions qualitatively similar to those in the molecule of **1**, but as Table 7 shows, they are much weaker. The pendant

nitrogen atoms in **3** are about the same distance away from the chromium atoms (the sum of the four CrCN distances is ca. 11.6 Å compared to 11.2 Å in **1**·THF and 11.6 Å in **1**·2THF) but the nitrogen lone pair orbitals are enormously more misdirected. In Cr<sub>2</sub>(dpa)<sub>4</sub> the sum of the direction angles varies from 104° to 124°, depending on the crystal form, whereas in **1**·THF and **1**·2THF these values were 12° and 23°, respectively. Thus, we would expect that for **3** the Cr–Cr bond lengthening effect would be relatively small and it is (0.07 Å), whereas in **1** it rises as high as 0.40 Å.

**Concluding Remarks.** The work reported here addresses (definitively in our opinion) the question of how axial interactions which inject electron density largely, if not entirely, into the  $\pi^*$  orbitals affect the Cr–Cr distance. It is clear that the effect can be very large (ca. 0.4 Å), or smaller, depending on how well placed and oriented the donor atoms are.

**Acknowledgment.** We are grateful to the National Science Foundation for financial support.

**Supporting Information Available:** Tables of crystallographic data including diffractometer and refinement data, atomic coordinates, bond lengths, bond angles, and anisotropic displacement parameters (PDF). An X-ray crystallographic file, in CIF format, is also available. This material is available free of charge via the Internet at <http://pubs.acs.org>.

JA9912675